



**HAL**  
open science

## Experimental Design of Solar DC Microgrid for the Rural Electrification of Africa

Lucas Richard, David Frey, Alexis Derbey, Marie-Cécile Alvarez-Herault,  
Bertrand Raison

► **To cite this version:**

Lucas Richard, David Frey, Alexis Derbey, Marie-Cécile Alvarez-Herault, Bertrand Raison. Experimental Design of Solar DC Microgrid for the Rural Electrification of Africa. PCIM Europe Nuremberg 2022, May 2022, Nuremberg, Germany. hal-03670489v2

**HAL Id: hal-03670489**

**<https://hal.science/hal-03670489v2>**

Submitted on 5 Jul 2022

**HAL** is a multi-disciplinary open access archive for the deposit and dissemination of scientific research documents, whether they are published or not. The documents may come from teaching and research institutions in France or abroad, or from public or private research centers.

L'archive ouverte pluridisciplinaire **HAL**, est destinée au dépôt et à la diffusion de documents scientifiques de niveau recherche, publiés ou non, émanant des établissements d'enseignement et de recherche français ou étrangers, des laboratoires publics ou privés.

# Experimental Design of Solar DC Microgrid for the Rural Electrification of Africa

Lucas Richard<sup>1,2</sup>, David Frey<sup>1</sup>, Alexis Derbey<sup>1</sup>, Marie-Cécile Alvarez-Herault<sup>1</sup>, Bertrand Raison<sup>1</sup>

<sup>1</sup> Univ. Grenoble Alpes, CNRS, Grenoble INP\*, G2Elab, France

<sup>2</sup> Nanoé, France

Corresponding author: Lucas Richard, lucas.richard@g2elab.grenoble-inp.fr

## Abstract

DC microgrids are a promising and cost-effective solution for the rural electrification of Africa or South-East Asia. However, microgrids mainly rely on power electronic converters and those converters must offer, in addition to their normal usage, protection and start-up services as well as low voltage ripple. This must be considered when designing converters for such particular applications. Moreover, field deployment of DC microgrids in rural places is often expensive and logistically difficult. Hence, it is necessary to develop a test bench to test and thoroughly validate the proper operation of a microgrid before its deployment. This paper presents the experimental design needed, from the converter to the test bench, to develop and deploy solar DC microgrids with decentralized production and storage for the rural electrification of Africa.

## 1 Introduction

Nowadays, almost one billion people have no or limited access to electricity in the world despite the United Nations (UN) Sustainable Development Goals of ensuring universal access to reliable and modern energy services by 2030 [1], [2]. The vast majority of those people resides in rural places in Sub-Saharan Africa or South-East Asia, where abundant resources of solar energy are available [1]–[3]. Electrifying such rural places through national grid extension is most of the time economically unviable as it requires large upfront costs for cable connections [3], [4]. On the other hand, Solar Home Systems (SHS), i.e. individual solar kits, are undoubtedly gaining momentum in rural places [3], [5] but they are only a stopgap measure to quickly give access to basic electricity services to the population. Low-energy access is often combined with high unemployment rate and poor local economic development [6], which can not be dealt with SHS. Therefore, to tackle the energy access challenge, it is highly crucial to propose an electrification model which can combine a quick and low-cost access to electricity to inhabitants of rural places and a community uplift through economic development. For instance, Nanoé, a French-Malagasy social company created in 2017, proposes an electrification

model based on the construction of electric infrastructures in a bottom-up manner while creating numerous local electric operators [6]. Nanoé installs and operates solar DC nanogrids (NG), consisting of one solar panel and one lead-acid battery for 4 to 6 houses. Those NGs, a low-cost solution easy to deploy, are only a first step in Nanoé's electrification model. In villages where multiple NGs are already installed, it is now highly relevant to interconnect them to form a microgrid (MG) to enhance electricity services, reduce hardware costs and offer productive use of electricity in rural places [4], [5], [7]–[9].

There is definitely a strong interest for AC and DC solar MGs in the rural electrification sector [4], [5], [9]–[11]. However, the topology of such MGs still remains an open question [12]–[14]. It is the belief of the authors that a fully decentralized DC topology is preferable, with decentralized production and storage, as advocated by the swarm electrification concept [5]. Such topology offers a scalable and modular way of building electric infrastructures in a bottom-up manner while being economically viable. In addition, decentralized DC MGs present lower upfront costs and lower losses than centralized topologies [4], [7], [13].

However, such DC MG entirely relies on power electronic converters and their control. It is therefore

\*Institute of Engineering Univ. Grenoble Alpes

needed to develop converters which are suited to those particular applications. There are many types of converters proposed for rural electrification, as the bidirectional buck-boost DC-DC converter [15] or more complex converters (Triple Active Bridge (TAB), flyback) [7], [16]. A converter designed for DC MGs must offer, in addition to its normal usage, protection and start-up services to facilitate the operation of the MGs. Moreover, ripple reduction is particularly important for the stability of the DC bus of the MG as voltage oscillations might interfere with the control algorithms of the MG [17].

An important constraint of rural electrification projects is that field deployment of DC MG pilots in rural areas is often logistically complicated, expensive and time-consuming. Therefore, it is crucial to develop extensive test benches in the lab to thoroughly test the operation of the proposed MGs before any test on the field. This necessitates fast and robust prototyping in the lab to be able to quickly validate a proposed structure without long engineering development time.

This paper proposes an experimental design, from the power converter to the test bench, to thoroughly test and validate the proper operation of a DC MG with decentralized storage and production before any field deployment. To the knowledge of the authors, only a few research institutes have designed a test bench for DC MG for rural electrification ([7], [8], [18] at the Center For Research on Microgrids (CROM) facilities and [9] at the University of Manitoba) and none have had the opportunity to deploy the proposed MG on the field.

The rest of the paper is organized as follows. Section 2 presents the design of a converter for a DC MG application. Section 3 details the development of a test bench for the proposed DC MG while section 4 describes the results of the converter and the test bench. Section 5 concludes and quickly introduces the field-test prototype of the converter.

## 2 Converter Design for Rural Electrification

### 2.1 DC Microgrid with Decentralized Production and Storage

The objectives of interconnecting NGs to form a DC MG are manifold. By mutualizing installed production and storage capacities, such a MG would use more efficiently hardware resources, improve the

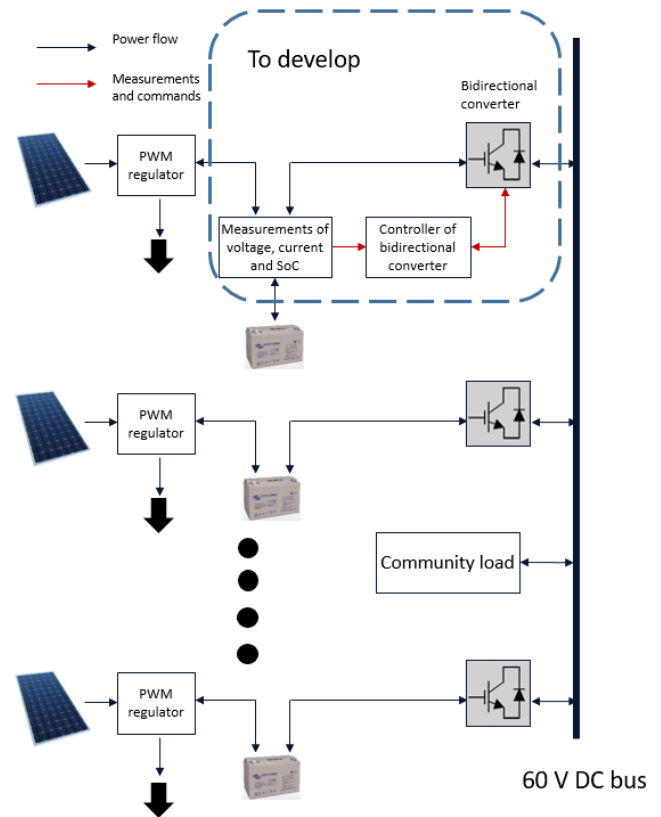


Fig. 1: Topology of the proposed microgrid.

lifetime of the batteries and offer higher electrical services to the community [4], [7], [8]. Overall, this would improve the economic viability and sustainability of such projects and help households and communities progressively climb the energy ladder [5], which would facilitate rapid scaling of those energy-access solutions.

The proposed MG interconnects all NGs in a close area to a 60 V DC bus through bidirectional DC-DC converters, as shown in Fig. 1. Communal loads such as rice huller or water pump can connect to the DC bus and be powered by all NGs. The control algorithm of the converter must be decentralized and communication-free to avoid a single point of failure and be affordably deployable even in areas where telecommunication signals are inexistent or unreliable [7]–[9]. Moreover, a decentralized and communication-free control algorithm enables plug and play features for the MG [9], which means that each NG can connect or disconnect to the MG without impacting the operation of the rest of the MG.

Therefore, based only on local measurements, the converter controls the power flows between the NG and the MG, i.e. if it must inject or absorb current on the DC bus. A converter assesses the energy state

**Tab. 1:** Parameters of the converter and the test bench.

Parameters	Symbol	Value	Parameters	Symbol	Value
Number of arms	$N$	2	Reference voltage of the MG	$V_{ref}$	60 V
Power inductor	$L_1, L_2$	360 $\mu$ H	Maximum voltage deviation of the MG	$V_{min}, V_{max}$	54 V, 66 V
DC bus capacitance	$C_{MG}$	3 mF	High threshold of the battery SoC	$SoC_{max}$	80%
Rated current	$I_{rated}$	18 A	Low threshold of the battery SoC	$SoC_{min}$	60%
Input voltage	$V_{bat}$	10-29 V	Lineic resistance of the electric cable	$R_l$	1.465 $\Omega/km$
Power rating	$P_{conv}$	500 W	Lineic inductance of the electric cable	$L_l$	337 $\mu$ H/km
Switching frequency	$f_{sw}$	25 kHz	Proportional and integral parameters	$k_p, k_i$	0.005, 0.001
Number of converters	$N_c$	3	PI integration step	$\delta t$	200 $\mu$ s

of the NG by measuring the State-of-Charge (SoC) of its battery, and the MG energy state with the DC bus voltage, which represents the global SoC of the MG, i.e the higher the voltage, the more globally charged is the MG and vice versa. High and low limits ( $\pm 10\%$ ) are set on the DC bus voltage. Figure 2 shows the proposed control algorithm, which ensures relevant and consistent power flows on the MG while maintaining the DC bus voltage within a certain range [7], as will be shown in Section 4.2. 3 regions can be defined for the energy state of the NG according to its battery SoC, i.e. low for SoC below 60%, medium for SoC between 60% and 80% and high for SoC above 80%, as defined in Table 1.

## 2.2 Fast Prototyping of a DC-DC Converter

A central element of the DC MG proposed is therefore the bidirectional DC-DC converter interfacing a 12 or 24 V NG to the 60 V DC bus. It has to be highlighted here that rural electrification projects often run on tight budgets and need fast results. Moreover, protection services and start-up procedure are necessary for the proper operation of the MG and it is economically interesting to directly include them in the bidirectional converter. For all those reasons, it has been chosen to design and use a bidirectional buck-boost converter for the proposed MG. Indeed, without galvanic isolation needed, a bidirectional buck-boost converter offers the best compromise between cost, ease and time of design and possible additional services. A bidirectional boost converter would have been sufficient for this application but for start-up procedure and network issues mitigation, a buck-boost topology is preferred, as shown with the schematics of the

converter in Fig. 3.

For protection services, mosfets Q1 and Q5 are necessary. Indeed, without mosfets Q1 and Q5, the NG would always be connected to the MG through the diodes of mosfets Q3 and Q7. To properly disconnect the NG to the MG, mosfets Q1 and Q5 must be opened. In addition, Q2 and Q6 are useful to offer a free-wheel path to the current in the inductors  $L_1$  and  $L_2$  in case of over-current and thus limit the constraints on the interface semiconductors (Q1, Q3, Q5, Q7).

Moreover, for start-up procedure, the arms Q1/Q2 and Q5/Q6 could be useful. As the DC bus contains high capacitors to stabilize the DC bus voltage and offer some inertia, the initial current at the start-up of the first converter can be high to charge all the capacitors to the desired voltage. Therefore, a start-up procedure, where the capacitors on the MG side of the converters are slowly brought to the input voltage thanks to the converter operating in buck mode, might be useful to limit the initial inrush current. Once the output voltage close to the input voltage, the converter can switch to boost operation to bring the DC bus voltage to its normal value.

In addition, under-voltage events on the MG could happen following a fault or a problem with a communal load (high transient current, DC motor suddenly blocked, etc.). If the DC bus voltage suddenly drops to a lower value than the NG voltage, a boost structure would fail due to the presence of the body diode of Q3 and Q7. Such events could therefore not be managed with only a boost converter whereas a buck-boost converter could switch to buck conversion to overcome the under-voltage event or disconnect the NG to the MG by opening Q1 and Q5. Lastly, in anticipation of future usages or features of the MG (e.g. communal loads, higher

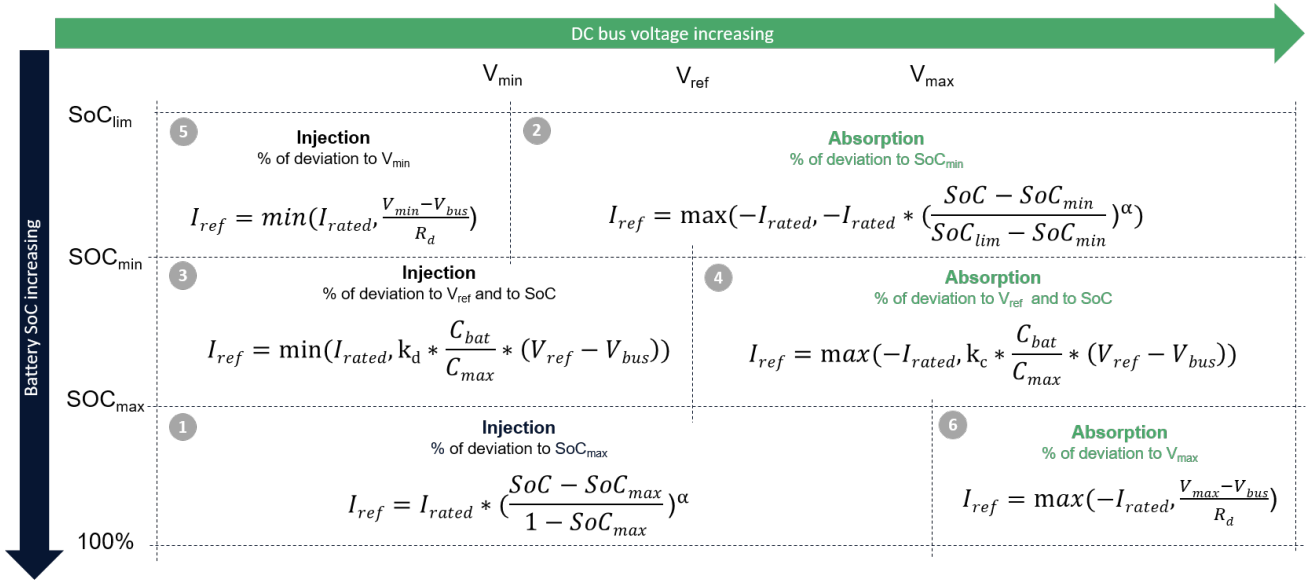


**Fig. 2:** Control algorithm of a converter interfacing a NG to the MG.

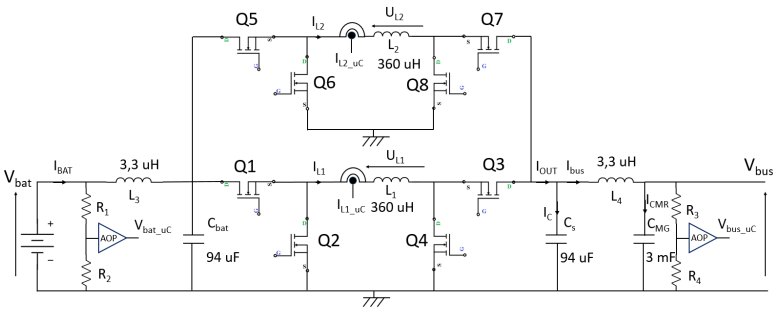


**Fig. 3:** Schematic of the proposed converter.

voltage range of operation), it is of interest to keep the buck operation mode available. By integrating those protection and start-up features, this topology permits to avoid to add costly electromechanical components such as circuit breakers or pre-charge relays to the system which normally perform those functions. Furthermore, as the control algorithm for the converter relies on the DC bus voltage, it is important to obtain low voltage ripple on the DC bus for stability purposes [7], [17]. Therefore, an interleaved converter with 2 arms is chosen to reduce voltage oscillation. Additional CEM filters and a high capacitive bus on the MG side are also included to further reduce voltage oscillations, increase inertia and reinforce stability. For a first prototype, 2 arms were considered to be a good compromise between design simplicity and ripple reduction. Multiple arms also enable modularity and can increase efficiency (only one arm used at low power to decrease switching losses for instance). In addition, it reduces the

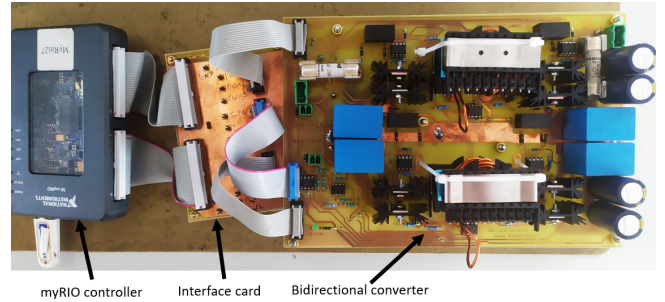


**Fig. 4:** Lab prototype of the proposed converter.

current per arm for a specified power rating, which eases the design of the power inductors, the rating of the mosfets and the thermal management of the entire converter. The designed converter can be seen in Fig. 4. As a first step, a prototype mock-up has been conceived in the lab. It is a 18 A converter (9 A per arm), current-controlled with a current sensor in each arm. Its input voltage range is 10 to 29 V (one or two batteries in series), hence it is a 500 W converter. Table 1 gathers information about the proposed converter. The converter is controlled through a myRIO embedded controller from National Instruments programmed in LabVIEW [19], as it can be seen in Fig. 4. The PWM signals driving the mosfets of the converter are generated by the FPGA module of the myRIO, at a frequency of 25 kHz whereas the microprocessor deals with the control algorithm of the converter and the PI regulation.

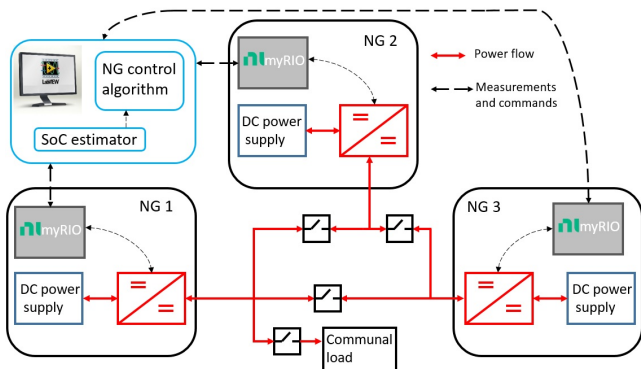


**Fig. 5:** Schematic of the proposed test bench.

### 3 Experimental Test Bench of a DC Microgrid

To validate and further tune the proposed DC MG, it is needed to develop a test bench for thorough testing of the operation of the MG. The objective of the test bench is to create a lab environment as close as possible from the real field conditions, with additional safety, monitoring, ease of installation and testing capacities. The schematic of the test bench is shown in Fig. 5 and the real test bench can be seen in Fig. 6. The test bench represents a MG with 3 NGs connected to each other and consists of 3 bidirectional buck-boost converters connected to a DC bus through RL lines. Each converter is controlled by one myRIO embedded controller. A power supply in parallel to an electronic load can be placed at the input of each converter to emulate a battery with additional features (current and voltage monitoring and current limitation). The RL lines emulate the impedance of the electric cables which would link the NGs, with 4 different available distances (20, 40, 60 and 80 meters) and the cabling set-up can be reconfigured easily as indicated in Fig. 5. A communal load can also be included with a power resistor.

The myRIOs enable to implement many different control features for the DC MG through the LabVIEW software and they are connected to a computer for communication and monitoring purposes. Firstly, the control algorithm of the proposed DC MG (shown in Fig. 2) is implemented on each myRIO. At each converter, the embedded myRIO controller associated measures the current and output voltage of the converter, i.e. the DC bus voltage, then runs the control algorithm which outputs the current reference for the converter. A numeric PI regulator is integrated in the Real-Time module of

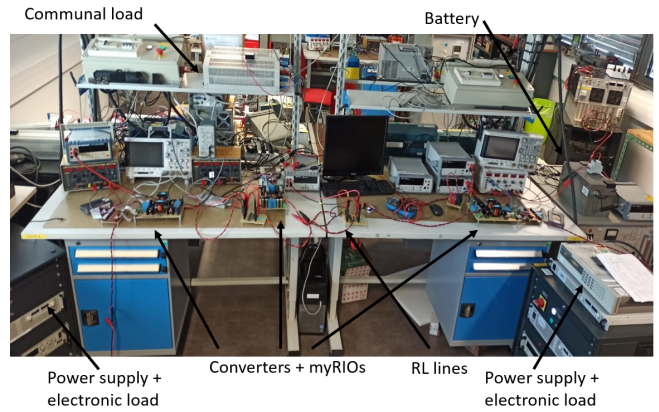


**Fig. 6:** Test bench of the proposed microgrid.

LabVIEW to control the duty cycle of the mosfets to regulate the current to its reference. Protection features are also included in the myRIOs, which open all high-side mosfets and close all low-side mosfets if any problems occur (such as over-current or over-voltage). In addition, the SoC of the NGs can be emulated on the myRIOs to test different operating points of the MG. The SoC can be automatically changed following a pre-defined scenario or manually changed through a Graphic User Interface (GUI). It is then possible to implement different production/consumption patterns for the NGs, and by using a very small capacity for the emulated batteries, SoC variation due to production/consumption patterns of the NGs can be emulated even on a short timeframe. Lastly, each myRIO records data every 25 ms (voltage, current, current reference, etc.). Therefore, post-treatment of the operation of the test bench is possible, which makes it very insightful. Table 1 summarises the different parameters of the developed test bench.

It must be highlighted here that the myRIO embedded controller and labVIEW permit fast prototyping by saving long engineering time associated with the use of micro-controllers and by enabling the implementation of numerous features on the test bench within a relatively small development time. This is believed to be particularly useful for this rural electrification project where the actual goal is to deploy a DC MG on the field and where the test bench is only a intermediary step to validate the proper operation of the proposed MG. Once a proof of concept has been given through a test bench in a lab, it is then relevant to go from a myRIO controller to a micro-controller.

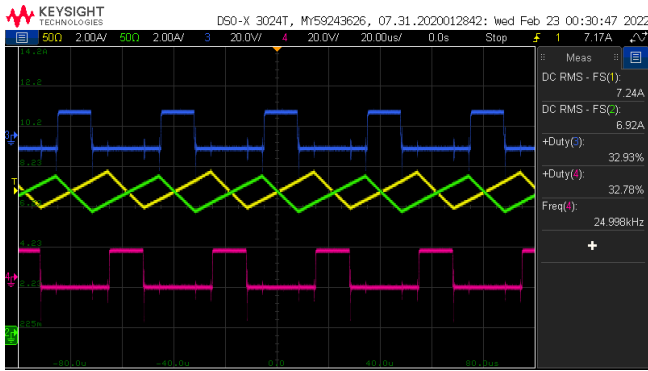


**Fig. 7:** PWM commands and inductor currents of both arms.

## 4 Experimental Results

### 4.1 Converter Performances

The converter can operate with one arm or 2 arms interleaved, with the PWM signals of both arms shifted of  $180^\circ$ , as can be seen in Fig. 7. The blue and pink signals show the PWM commands of mosfets Q3 and Q7 whereas the green and yellow signals show the current in power inductors  $L_1$  and  $L_2$ . The currents are shifted by  $180^\circ$  so the output current ripple and then the output voltage ripple are reduced, which is useful for the stability of the control algorithm. It can be noted that the RMS values of both currents are not exactly equal due to small measurement errors which impede the PI regulators of each arm to achieve exact current sharing.

Figure 8 shows the efficiency of the proposed converter for different cases, i.e. one or two arms and 12 or 24 V NG. A higher efficiency is obtained with 24 V NGs than with 12 V NGs, which proves that the main losses are due to conduction losses. For a certain input power, the current will be divided by 2 between a 12 V NG and a 24 V NG which would reduce the conduction losses per a factor around 4 and then increase the efficiency of the converter. As the switching frequency is only 25 kHz, the switching losses are relatively negligible. Also, at a certain power, at a certain voltage (12 or 24 V), there is two times less current in the power inductors with two arms than with one arm. As the conduction losses are quadratic with the current, the efficiency is higher with two arms than with one arm, even at the same voltage, which is confirmed by Fig. 8. With a higher switching frequency and a lower current per arm, this might not be the case and then using only one arm instead of two arms

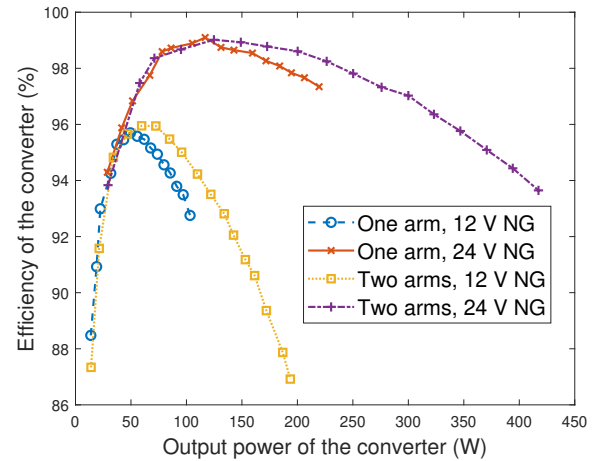


**Fig. 8:** Efficiency of the converter for different cases of usage.

might be relevant to increase efficiency (by turning off one arm, the switching losses of this arm would be 0). Overall, the converter obtains high level of efficiency, especially with two arms with a 24 V NG (up to 99%), which is highly satisfying. If the average operating point of the converter exceeds 150 W, it becomes relevant to change to a 24 V NG to increase the efficiency of the converter. However, it remains an open question whether such a high efficiency traduces or not a global optimum for the design of the converter and the proposed converter does not claim to be perfectly sized. Additional work will be needed in the future to optimise the proposed converter.

On the MG, the first converter to be launched must charge all the DC bus capacitance to the operating voltage. Figure 9 and 10 show the inrush current from the battery and the DC bus voltage when starting a converter respectively in boost mode and in buck then boost mode. This is done with a 90 Ah lead-acid Victron battery charged at 13 V and with only one converter connected to the DC bus. The start-up procedure consists of starting in buck mode to slowly bring the DC bus to a voltage close to the NG voltage, then switch to boost mode. It can be seen that when starting directly in boost mode, the initial inrush current reaches almost 40 A and is quite important for 2 ms whereas when starting in buck mode there is only a 400 mA peak at the beginning in buck mode (as shown by the part zoomed in of Fig. 10) and a 1 A peak at the end of the boost mode, which starts approximately 150 ms after the buck mode. Note that there is a ratio of 40 between the current scales of both figures. The



Fig. 9: Initial inrush current without start-up procedure.

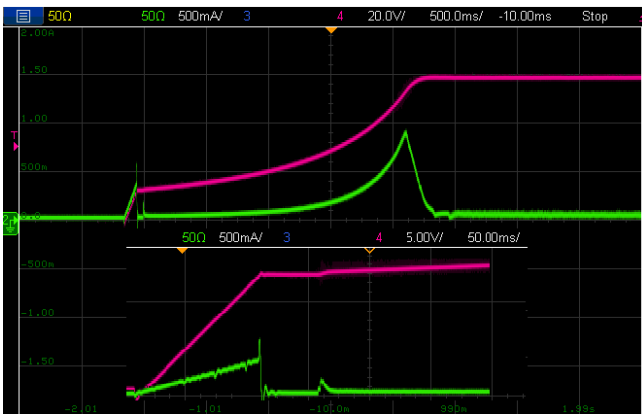


Fig. 10: Initial inrush current with start-up procedure.

start-up procedure enables to control the current in the buck mode until the DC output voltage reaches close to the NG voltage. Without this start-up procedure, the current can not be controlled until the DC output voltage reaches the input voltage. The initial inrush current without start-up procedure would be even worse with additional capacitance on the DC bus (i.e. with more converters connected to the DC bus) and with a 24 V NG.

Furthermore, when a converter starts with an already existing MG (i.e. an other converter is already launched), it is crucial that the converter starts at the proper duty cycle, i.e.  $V_{bat}/V_{bus}$  to avoid any high initial current. Different tests have been carried out with a 12 V NG and a 60 V MG (i.e. a proper duty cycle of 20%) and high initial inrush currents have been observed when starting with a duty cycle different from 20%. The converter can even fail and break with an initial duty cycle too far from 20%, which proves that this precaution is essential.

Moreover, protection features of the power converter have been thoroughly tested. In case of overcurrent, overvoltage or undervoltage events,

the converter reacts by opening Q1 and Q5 and closing Q2 and Q6 (creating a free-wheel path), separating the NG to the MG and discharging the magnetic energy of the inductors within their own resistance. Manual interruption of the converter has also been tested while operating at high power levels, with satisfying results. The protection procedure of opening Q1/Q5 and closing Q2/Q6 enables to limit the constraints on the interface semiconductors, which is believed to preserve the lifetime of those components.

The results shown here enable to affirm that the proposed converter presents satisfying performances and that the proposed topology does permit additional protection and start-up features, which is particularly relevant for DC MGs.

## 4.2 Power Flows on the DC Microgrid

The test bench enables to study the operation of the MG. More precisely, the power flows between the different batteries, depending on their SoC level, can be observed as well as the variation of the DC bus voltage. Figure 11 shows the evolution of the DC bus voltage, the emulated SoCs of the 3 batteries and the currents exchanged between the batteries at different operating points. Note that when the current on the NG side is positive, it means that the NG is injecting current on the MG and vice versa. In this scenario, the SoCs are automatically evolving according to different production/consumption patterns implemented in labVIEW. It is important here to remind that a converter determines whether it must inject or absorb current according to the SoC of its NG and the DC bus voltage, as described in Fig. 2. It can be seen that NG 2 starts to inject current to the MG (at  $t=60$  s) as the DC bus voltage is very low and its SoC reaches 60%, and then supports NG 1 and NG 3. As the SoC of the 3 NGs are evolving, the amount of exchanged current reduces to 0 A ( $t=190$  s) when NG 1 and NG 3 reach a SoC of 60%. The DC bus voltage is then stabilized at 60 V which indicates that the global energy level of the MG is medium (i.e., all the batteries have a SoC at a medium level as defined in Section 2.1). Then, due to its production/consumption pattern, NG 2 reaches first a SoC above 80% and starts to inject current to the MG (at  $t=220$  s), supporting NG 1 and 3, until they reach 80% of SoC (at  $t=470$  s). The voltage then stabilizes at 66 V, indicating that the MG is at a high level (i.e., all the batteries have a SoC at a high level). It is interesting to note that

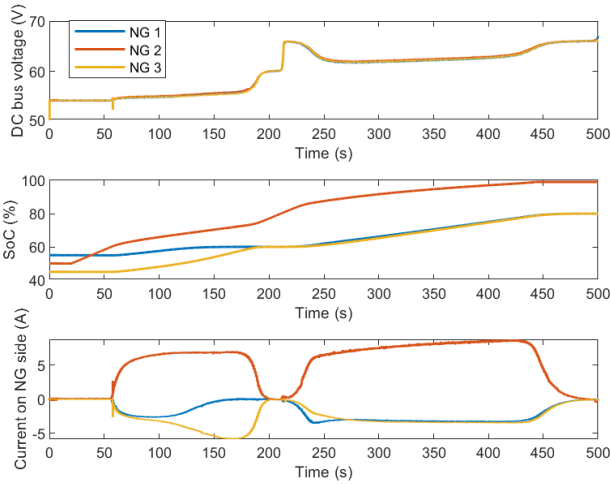


**Fig. 11:** Evolution of the voltage, the SoCs and the currents exchanged between the batteries on the test bench.

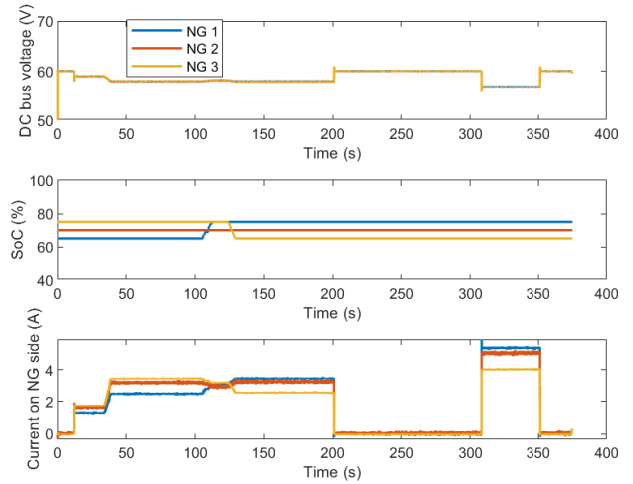


**Fig. 12:** Evolution of the voltage, the SoCs and the currents with the introduction of a communal load on the DC bus.

when NG 2 starts to inject current at  $t=220$  s, the DC bus voltage shortly stabilizes at 66 V because NG 1 and NG 3 did not respond quickly enough to the increase in voltage. This is due to an inherent delay of the electronic loads used in the test bench when the currents are low. They start to absorb current a few seconds after they should have which makes the DC bus voltage increase momentarily.

Figure 12 shows the operation of the MG with a communal load. The 3 batteries are charged between 60% and 80%, hence the DC bus voltage is at 60 V. At  $t=10$  s, a communal load (i.e. a power resistor in this case) is connected to the DC bus, its power consumption being increased from  $t=30$  s to  $t=40$  s. It is then disconnected at  $t=200$  s and reconnected at  $t=310$  s with a greater power. The 3 batteries inject current in proportion to their SoC level, the greater the SoC, the more current injected. Around  $t=110$  s, the SoCs of the NG 1 and 3 are manually modified to highlight this current sharing feature. Lastly, the DC bus voltage does change with the loading of the communal load, i.e. the greater the power of the communal load, the lower the DC bus voltage. This is logical with the fact that when powering a high power communal load, the MG has in average less energy reserve, hence its DC bus voltage is lower. The operation of the MG with a communal load is satisfying and validated with the results shown in Fig. 12.

Many other tests have been successfully carried out (different topologies, meshed, radial, length of lines, etc.) and the results obtained permit to affirm

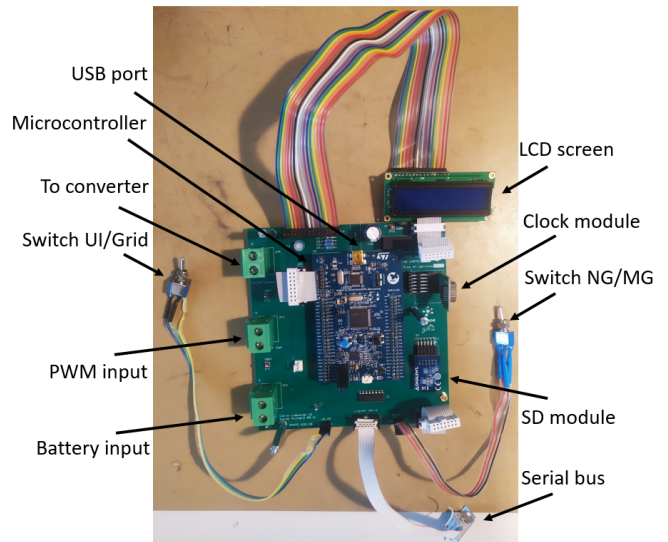


**Fig. 13:** Command card of the interconnection module.

that the proposed DC MG is operating well and that the proposed control algorithm enables consistent power flows while guarantying stability of the MG and maintaining the DC bus voltage within a certain range. It can also be confirmed here that the DC bus voltage does translate in the average energy situation of the MG. This is useful for the use of communal loads or for future interconnections to other MGs or to the national grid [5], [9]. For instance, the time at which communal loads are powered could be decided with the DC bus voltage level or the amount of power exchanged between two connected MGs could depend on their respective DC bus voltage level.

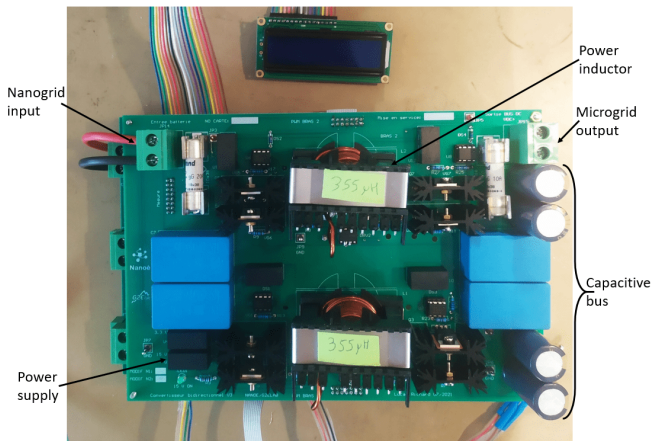


Fig. 14: Power card of the interconnection module.

## 5 Conclusion

This paper presents the development of a DC-DC converter suited for DC MG with decentralized storage and production as well as a test bench of the proposed MG. Performances of the converters and the operation of the test bench are presented in details.

The successful lab prototype of the converter presented here has led to the design of a field-test prototype of an interconnection module, designed to operate autonomously on the field for a long period of time. For practical reasons, additional functionalities have been added to the interconnection module such as LCD screen, SD module, clock, User Interface (UI), as can be seen in Fig. 13 and 14. The interconnection modules have then been installed on the field in Madagascar at the end of 2021 to interconnect 5 NGs and are successfully running since then.

This work is only a first step in a design method for power converters suited to their application and future works will focus on thorough study of co-design between the MG and the converter. In particular, as the MG is still under development and open to changes, it is particularly interesting to assess how the MG specifications and the converter design are intertwined to find a techno-economic optimal of the MG/converter system. The second version of the interconnection module will fully take into account those considerations.

## Acknowledgements

This research, a part of the LEAP-RE project, was funded by the European Union's Horizon 2020 re-

search and innovation program under grant agreement N° 963530. This paper reflects only the authors' view and the European Climate, Infrastructure and Environment Executive Agency and the European Commission are not responsible for any use that may be made of the information it contains.



## References

- [1] "United Nation 17 Goals." (2021), [Online]. Available: <https://sdgs.un.org/goals>.
- [2] "World Energy Outlook (WEO, 2021)." (2021), [Online]. Available: <https://www.iea.org/reports/world-energy-outlook-2021>.
- [3] M. Moner-Girona, K. Bódis, J. Morrissey, I. Kougias, M. Hankins, *et al.*, "Decentralized rural electrification in Kenya: Speeding up universal energy access," *Energy for Sustainable Development*, vol. 52, pp. 128–146, 2019.
- [4] M. Nasir, H. A. Khan, N. A. Zaffar, J. C. Vasquez, and J. M. Guerrero, "Scalable solar DC microgrids," *IEEE Electrification Magazine*, vol. 6, no. 4, pp. 63–72, 2018.
- [5] S. Groh, D. Philipp, B. E. Lasch, and H. Kirchhoff, *Swarm Electrification: Investigating a Paradigm Shift Through the Building of Microgrids Bottom-up*, 2015.
- [6] "Nanoé presentation website." (2021), [Online]. Available: <https://www.nanoe.net/en/>.
- [7] M. Nasir, Z. Jin, H. A. Khan, N. A. Zaffar, J. C. Vasquez, and J. M. Guerrero, "A Decentralized Control Architecture Applied to DC Nanogrid Clusters for Rural Electrification in Developing Regions," *IEEE Transactions on Power Electronics*, vol. 34, no. 2, pp. 1773–1785, 2019.

- [8] M. Nasir, M. Anees, H. A. Khan, and J. M. Guerrero, "Dual-loop control strategy applied to the cluster of multiple nanogrids for rural electrification applications," *IET Smart Grid*, vol. 2, no. 3, pp. 327–335, 2019.
- [9] D. Li and C. N. M. Ho, "A Module-Based Plug-n-Play DC Microgrid with Fully Decentralized Control for IEEE Empower a Billion Lives Competition," *IEEE Transactions on Power Electronics*, vol. 36, no. 2, pp. 1764–1776, 2021.
- [10] E. O'Neill-Carrillo, I. Jordan, A. Irizarry-Rivera, and R. Cintron, "The long road to community microgrids: Adapting to the necessary changes for renewable energy implementation," *IEEE Electrification Magazine*, vol. 6, no. 4, pp. 6–17, 2018.
- [11] A. Jhunjhunwala, A. Lolla, and P. Kaur, "Solar-DC Microgrid for Indian Homes: A Transforming Power Scenario," *IEEE Electrification Magazine*, vol. 4, no. 2, pp. 10–19, 2016.
- [12] T. Dragicevic, X. Lu, J. C. Vasquez, and J. M. Guerrero, "DC Microgrids — Part II : A Review of Power Architectures, Applications, and Standardization Issues," vol. 31, no. 5, pp. 3528–3549, 2016.
- [13] M. Nasir, N. A. Zaffar, and H. A. Khan, "Analysis on central and distributed architectures of solar powered DC microgrids," in *2016 Clemson University Power Systems Conference (PSC)*, 2016, pp. 1–6.
- [14] S. Liptak, M. Miranbeigi, S. Kulkarni, R. Jinsiwale, and D. Divan, "Self-organizing nanogrid (SONG)," in *2019 IEEE Decentralized Energy Access Solutions Workshop (DEAS)*, 2019, pp. 206–212.
- [15] P. Shaw, P. K. Sahu, S. Maity, and P. Kumar, "Modeling and control of a battery connected standalone photovoltaic system," in *2016 IEEE 1st International Conference on Power Electronics, Intelligent Control and Energy Systems (ICPEICES)*, 2016, pp. 1–6.
- [16] C. Samende, N. Mugwisi, D. J. Rogers, E. Chatzinikolaou, F. Gao, and M. McCulloch, "Power loss analysis of a multiport DC - DC converter for DC grid applications," *Proceedings: IECON 2018 - 44th Annual Conference of the IEEE Industrial Electronics Society*, vol. 1, pp. 1412–1417, 2018.
- [17] T. Dragicevic, X. Lu, J. C. Vasquez, and J. M. Guerrero, "DC Microgrids — Part I : A Review of Control Strategies and Stabilization Techniques," vol. 31, no. 7, pp. 4876–4891, 2016.
- [18] M. Nasir, M. Anees, H. A. Khan, I. Khan, Y. Xu, and J. M. Guerrero, "Integration and Decentralized Control of Standalone Solar Home Systems for Off-Grid Community Applications," *IEEE Transactions on Industry Applications*, vol. 55, no. 6, pp. 7240–7250, 2019.
- [19] "LabVIEW presentation website." (2021), [Online]. Available: <https://www.ni.com/en-za/shop/labview.html>.